Available online at www.sciencedirect.com

SciVerse ScienceDirect

Ceramics International 38 (2012) 5637–5642

CERAMICS INTERNATIONAL

www.elsevier.com/locate/ceramint

Structures and temperature-dependent electrical properties in $Ba_{0.8}Sr_{0.2}TiO_3$–$BiAlO_3$ electrostrictive ceramics

Chong Zhang [a], Long Jiao [a], Huajun Kang [b], Zheng-Bin Gu [a], Guo-Liang Yuan [c], Jun Chen [b], Shan-Tao Zhang [a,*]

[a] Department of Materials Science and Engineering and National Laboratory of Solid-State Microstructures, Nanjing University, Nanjing 210093, China
[b] Department of Physical Chemistry, University of Science and Technology Beijing, Beijing 100083, China
[c] School of Materials Sciecne and Engineering, Nanjing University of Science and Technology, Nanjing 210094, China

Received 29 February 2012; received in revised form 1 April 2012; accepted 2 April 2012
Available online 11 April 2012

Abstract

Lead-free piezoceramics of $(1-x)Ba_{0.8}Sr_{0.2}TiO_3$–$xBiAlO_3$ [$(1-x)$BST–xBA ($0 \le x \le 0.12$)] have been synthesized and the structures and properties have been investigated systemically. X-ray diffraction patterns indicated that the solid solution limit is close to $x = 0.04$, and a morphotropic phase boundary (MPB) separating tetragonal and pseudocubic phases exists near $x = 0.02$. The ferroelectricity weakens monotonously with increasing x, accompanied by weakened butterfly shaped bipolar strain–electric field curves. The temperature dependent properties of the composition with $x = 0.02$ have been typically investigated, showing that with increasing temperature, the ferroelectricity tends to be weakened. Pure electrostrictive effect has been found in the compositions with $x = 0.02$ and 0.03 close to room temperature temperature. Based on the results, the effects of BA on structures and electric properties were discussed.
© 2012 Elsevier Ltd and Techna Group S.r.l. All rights reserved.

Keywords: $Ba_{0.8}Sr_{0.2}TiO_3$; $BiAlO_3$; Strain; Electrostrictive

1. Introduction

At present most widely used piezoelectric materials are lead-based, such as $Pb(Zr,Ti)O_3$ (PZT). The lead-based materials have applications in actuators, sensors, and transducers due to their excellent electromechanical properties [1]. However, lead is toxic and its use is banned in many commercial applications [2]. To replace lead-based piezoelectric materials, huge efforts have been devoted to the search for lead-free counterparts with comparable properties. At present no lead-free piezoelectric materials can display comparable properties. Therefore, an alternative way is suggested to classify the required piezoelectric properties for various applications and develop lead-free piezoelectric ceramics targeted for each application accordingly [3].

For actuator applications, the generally requirements is high strain because $e_{max} \propto s_{max}^2$, where e_{max} is the strain energy, s_{max} is the maximum field induced strain [1]. The common method to develop high strain materials is to form the morphotropic phase boundary (MPB) which generally shows improved strain [1–5]. However, the strain–electric field (S–E) curves of the reported MPB compositions still have hysteresis, which is detrimental for improving the fine position controlling, reducing energy consuming, etc., of electronic devices.

Actually, electrostrictive materials have hysteresis-free characteristics and, therefore, are of particular interest for actuator application [6]. But electrostrictive effect is very weak in most materials and the typical strain level is less than 0.10% [7]. However, in some relaxor ferroelectrics, the electrostrictive strain can reach 0.10–0.15%. Up to now, the reported lead-free electrostrictive materials are generally based on $Bi_{0.5}Na_{0.5}TiO_3$ [7,8]. One problem related with these BNT-based electrostrictive materials is that, extremely high field (larger than 8 kV/mm) is necessary to obtain ~0.1% strain level. The high field is one of the obstacles preventing its application. We note that recent theoretical and experimental works indicate modified $BaTiO_3$ (BT) based materials can also show electrostrictive effect with strain level of ~0.1% at low applied

* Corresponding author.
E-mail address: stzhang@nju.edu.cn (S.-T. Zhang).

0272-8842/$36.00 © 2012 Elsevier Ltd and Techna Group S.r.l. All rights reserved.
http://dx.doi.org/10.1016/j.ceramint.2012.04.006

electric field [9,10], which means that it might be interesting to search for BT-based electrostrictive materials.

Barium strontium titanate, $Ba_xSr_{1-x}TiO_3$, is a solid solution composed of barium titanate and strontium titanate. $Ba_xSr_{1-x}TiO_3$ has attracted much electronic interests mainly due to its high dielectric constant, alterable Curie temperature, low dielectric loss, high dielectric tunability, etc. Most of the reported works focused on the effects of Ba/Sr composition [11–16], etc., on dielectric properties, but few of them on its electrostrictive effect. It is noted that $Ba_{0.8}Sr_{0.2}TiO_3$ (BST) has been reported to have tetragonal phase, and especially, show strong relaxations in terms of frequency dependence of the dielectric properties [12,14]. That means electrostrictive effects might be observed in BST-based materials.

On the other hand, an increasing attention has been paid to $BiAlO_3$ (BA) due to its large spontaneous polarization. However, it is known that the extremely structural unstability has made BA difficultly available under normal conditions [17]. Moreover, its real crystal structure is still vague, it is being considered to own rhombohedral structure through theoretical calculations, but a tetragonal structure from experimentally prepared films [18]. Therefore, attempts have been made to stabilize BA by forming solid-solution with other stable perovskite materials, which results in a synergic effect that leads to a significant changes in structural and electrical properties [19,20].

Based on the above description, we have designed and prepared the solid solutions of $(1-x)$BST–xBA with $x = 0$, 0.01, 0.02, 0.03, 0.04, 0.06, 0.09 and 0.12. The solid solution limit, crystal structure, electrical properties and its temperature dependence have been investigated and discussed.

2. Experimental procedure

The $(1-x)$BST–xBA ($x = 0$, 0.01, 0.02, 0.03, 0.04, 0.06, 0.09 and 0.12) ceramics were prepared using solid-state reaction method. Oxide and carbonate powders of $BaCO_3$ (99.8%), $SrCO_3$ (99.8%), TiO_2 (99.9%), Bi_2O_3 (99.8%) and Al_2O_3 (99.0%) were used as starting materials. Before being weighed, these powders were separately dried in an oven at 60 °C for 24 h. For each composition, the oxides and carbonates were weighed according to the stoichiometric formula of $(1-x)$BST–xBA with $x = 0$, 0.01, 0.02, 0.03, 0.04, 0.06, 0.09 and 0.12. The mixtures were ball milled for 24 h in ethanol, the dried slurries were calcined at 900 °C for 3 h in air and then ball milled again for 12 h. The dried powders were pressed into disks of 10 mm in diameter under a uniaxial pressure of 40 MPa using polyvinyl alcohol (PVA) as a binder. The pellets were sintered at 1250–1350 °C for 3 h in sealed Al_2O_3 crucibles. For electrical measurements, the sintered disks were grounded carefully to ensure the parallel surfaces. The circular surfaces of the disks were covered with a thin layer of silver paste and fired at 500 °C for 30 min in air.

X-ray diffraction (XRD, Rigaku UltimaIII) and scanning electron microscope (SEM, XL30 Philips) were used for structure characterizations. The XRD measurements were carried on crushed, unpoled samples. The polarization–electric field (P–E) hysteresis loops and the strain–electric field (S–E) curves were measured by TF Analyzer 1000 (AixACCT, Germany) in silicone oil with controllable temperature.

3. Results and discussions

Fig. 1(a) shows the XRD patterns of the $(1-x)$BST–xBA ceramics. As can be seen, the ceramics have been crystallized to pure perovskite phase and no secondary phases can be identified when $x < 0.04$, indicating that the BA have completely diffused into the BST lattice to form solid solution. However, a second phases, indicated by the arrows and identified as $Bi_2Al_4O_9$ [10], tends to develop as $x \geq 0.04$. This means the solution limit is close to $x = 0.04$, which is significantly lower than that of $(1-x)BaTiO_3$–$xBiAlO_3$ system [20], one of the possible reasons is that BST and $BaTiO_3$, though have same tetragonal crystal structure, have different lattice parameter and thus different accommodation for introduction of rhombohedral metastable $BiAlO_3$. On the other hand, it is clear that with increasing x from 0 to 0.02, some diffraction peaks, e.g., that locating at $2\theta = 45.5°$ in Fig. 1(a), become coalesced. Typically detailed composition-dependent XRD patterns near $2\theta = 45.5°$ are plotted in Fig. 1(b). For the composition with $x = 0$ and 0.01, the diffraction peaks are split, which is the fingerprint of tetragonal structure. With x is increased to 0.02, these split peaks are coalesced into one peak with a weak shoulder at lower-angle side. With further increasing x, the shoulders tend to disappear, suggesting that the crystal structure of the $(1-x)$BST–xBA ceramics evolves from the tetragonal to a possible pseudocubic symmetry, in other words, a tetragonal-pseudocubic MPB locates near $x = 0.02$.

Fig. 2 typically shows the SEM micrographs of the $(1-x)$BST–xBA ceramics with $x = 0.01$, 0.02, 0.03, and 0.04. The SEM observations confirm that all samples are dense with well-developed microstructure and grain morphologies. The average grain size is about 1 μm. No significant composition dependent grain size and microstructural morphologies can be observed, though the composition with $x = 0.04$ has second phases, which might indicate that the ratio of second phases is very low.

Electrical measurements have been carried out on all samples, however, it is found the composition with $x = 0$ is

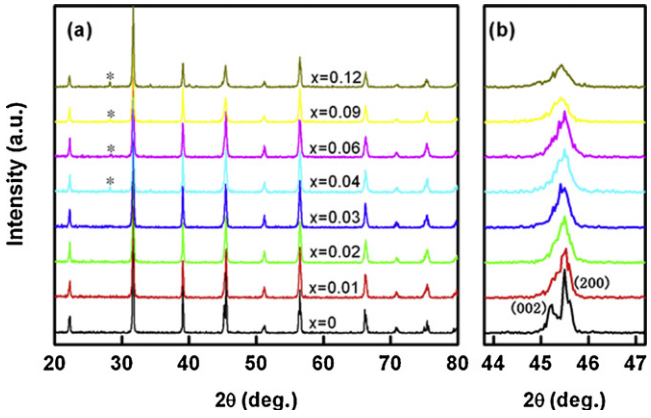

Fig. 1. (a) XRD patterns of all $(1-x)$BST–xBA ceramics. (b) The local detailed XRD patterns, showing a phase transition.

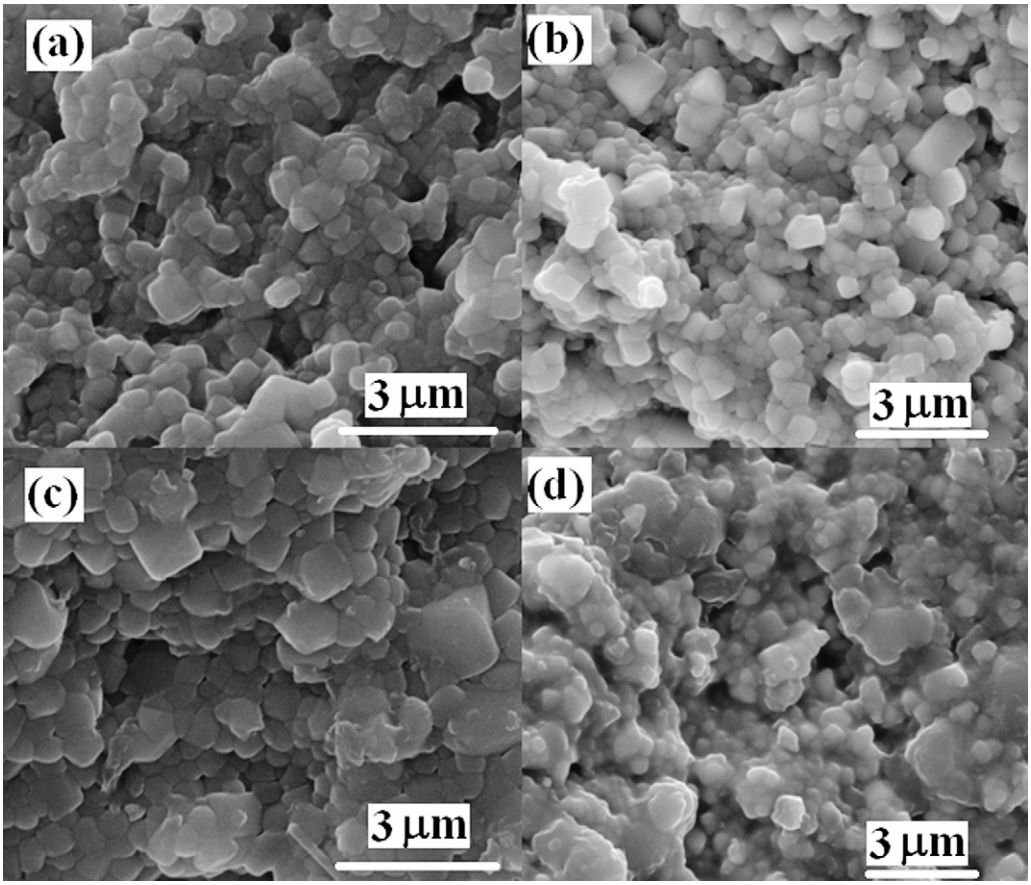

Fig. 2. Typical SEM images of samples (a) $x = 0.01$, (b) $x = 0.02$, (c) $x = 0.03$, and (d) $x = 0.04$.

electrically breakdown at very low field. By further considering that the compositions with $x \geq 0.04$ are not single phased, therefore, only electrical properties of the compositions with $x = 0.01$, 0.02 and 0.03 will be shown and discussed below.

As shown in Fig. 3, with an applied field of 10 kV/mm, the single phased ceramics show well saturated *P–E* hysteresis loops, indicating the ferroelectric nature. As can be seen, the compositions with $x = 0.01$ exhibits a better rectangle shaped loop than other compositions, or in other words, the loop tends

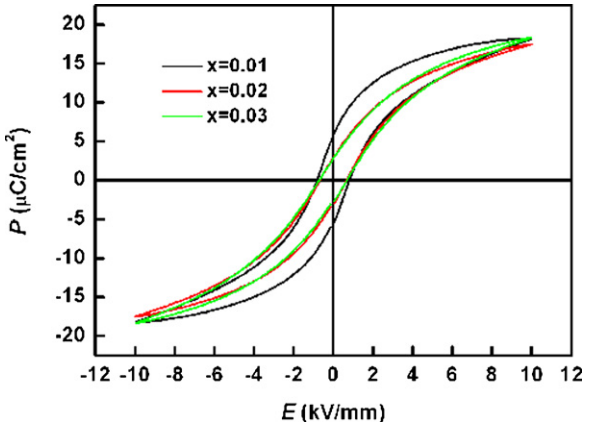

Fig. 3. The *P–E* hysteresis loops of the compositions with $x = 0.01$, 0.02, and 0.03.

to become slim with increasing x. The measured saturated polarization (P_s), remnant polarization (P_r) and coercive field (E_c) of the composition with $x = 0.01$ are 5.8 μC/cm^2, 18.1 μC/cm^2, and 0.8 kV/mm, respectively. As x increases, a decrease in P_s and P_r, and E_c can be observed. Similar slim loops have also been reported [22–26], which implies that the dominant ferroelectric order in BST is disrupted with the addition of BA, possibly because of the stabilization of a "weak" ferroelectric phase with a 'nonpolar' phase [23,27]. Based on these *P–E* loops and by further noting that pure BST is a relaxor ferroelectrics [21], it might be safe to conclude that the compositions with $x = 0.01$–0.03 are relaxor ferroelectrics.

It should be mentioned that the poled $(1 - x)$BST–xBA ceramics show very low or undetectable direct piezoelectric coefficient (d_{33}), even in the MPB region ($x \sim 0.02$). Actually, a MPB separating tetragonal/orthorhombic and pseudocubic phases generally have no enhanced piezoelectric properties, as being reported in $Bi_{0.5}Na_{0.5}TiO_3$-based solid solutions [28].

Fig. 4 shows the bipolar *S–E* curves of the $(1 - x)$BST–xBA ceramics with $x = 0.01$–0.03 measured at room temperature. Two features should be mentioned. Firstly, for the composition with $x = 0.01$, the negative strain, which is the strain between zero-field strain and the lowest strain and is the fingerprint of ferroelectric nature, is still detectable, whereas with increasing x, it tends to vanish, obviously for the composition with

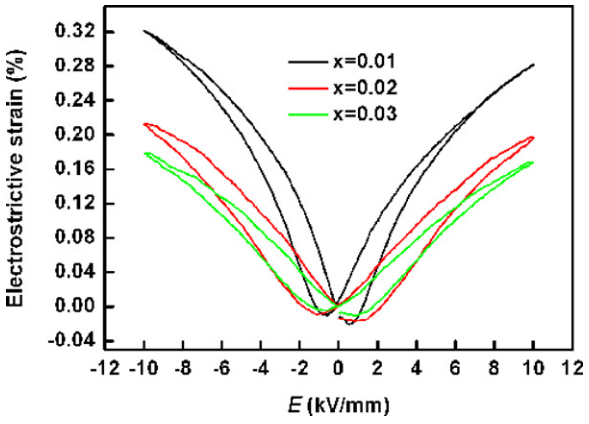

Fig. 4. Bipolar *S–E* loops of the compositions with $x = 0.01$, 0.02, and 0.03.

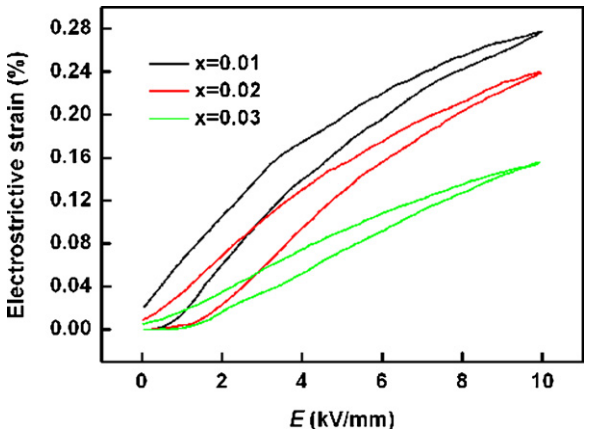

Fig. 5. Unipolar *S–E* loops of the compositions with $x = 0.01$, 0.02, and 0.03.

$x = 0.03$. In other words, the bipolar strain curves clearly confirm that the ferroelectricity weakens with the increasing of x, consistent with the *P–E* loops shown in Fig. 3. Similar results have been observed in $Bi_{0.5}Na_{0.5}TiO_3$-based ceramics [29]. Secondly, the measured maximum strains of the ceramics decrease from 0.32% to 0.21%, and then to 0.18% when x comes from 0.01 to 0.03. Beyond this region, the maximum strain drastically decreases, whereas the negative strain vanished completely. The decreased strain can be attributed to that the introduction of BA weakens the ferroelectricity by forming nonpolar phase [27], and thus the contribution of ferroelectric domain switching to strain decreases.

The unipolar *S–E* curves of $(1 - x)$BST–xBA ceramics measured at room temperature with $x = 0.01$–0.03 are plotted in Fig. 5. Similar with the bipolar strain curves, the strain decreased significantly with increasing BA content up to $x = 0.03$.

Fig. 6(a) shows the *P–E* hysteresis loops of $(1 - x)$BST–xBA ceramics with $x = 0.02$ measured under an electric field of 8 kV/mm at different temperatures. With the increasing temperature, a reduction in P_r and E_c are observed and the hysteresis loop becomes slim, possibly suggesting the formation of nonpolar phases [27]. On the other hand, bipolar and unipolar *S–E* curves show similar reducing of electrostrictive strain at different temperature in Fig. 6(b) and (c). More interestingly, the *S–P*^{2} curves measured at different temperatures are shown in Fig. 6(d), clearly, the *S–P*^{2} curves for the temperature from 75 °C to 100 °C are linear, indicating the pure electrostrictive effect with high strain level of 0.16%, whereas that at room temperature there is detectable hysteresis

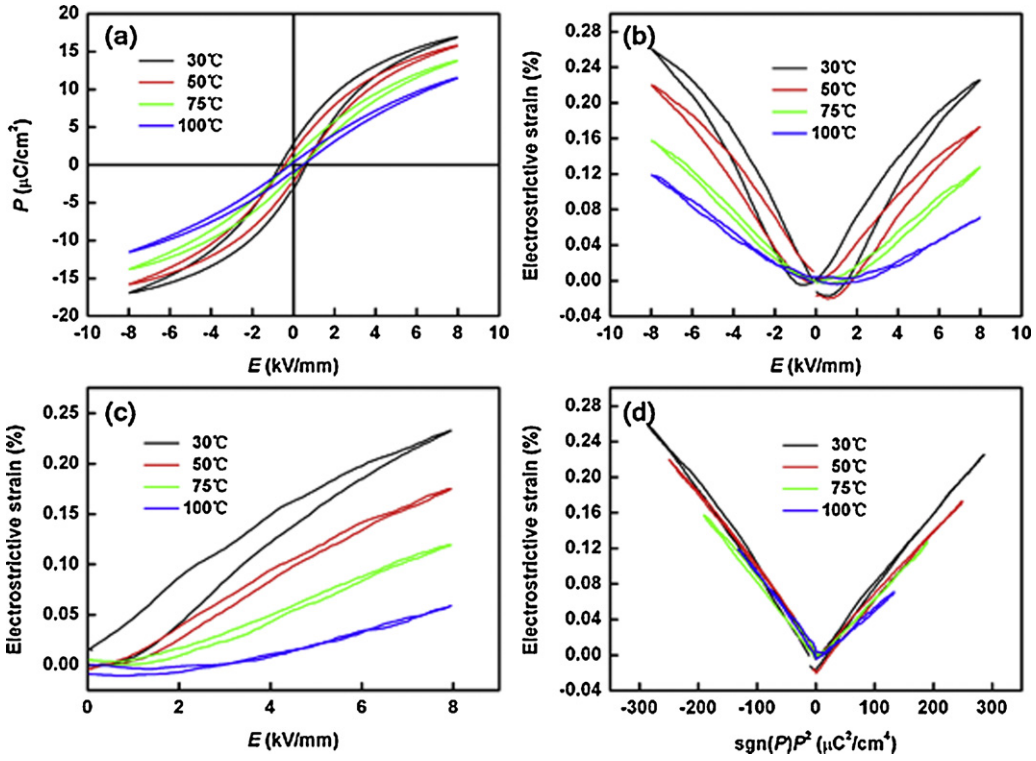

Fig. 6. (a) *P–E* loops, (b) bipolar *S–E* curves, (c) unipolar strain *S–E* curves, and (d) *S–P*^{2} curves of the composition with $x = 0.02$ at different temperatures.

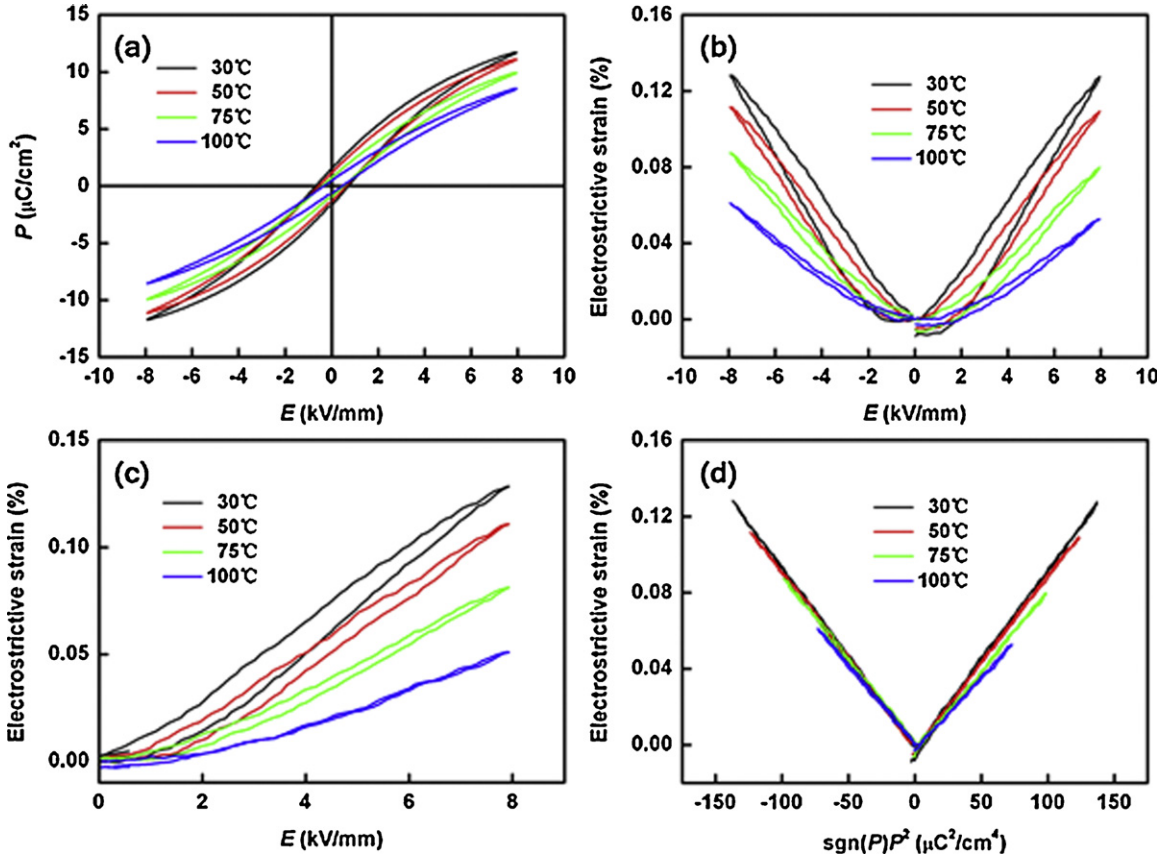

Fig. 7. (a) P–E loops, (b) bipolar S–E curves, (c) unipolar strain S–E curves, and (d) S–P^2 curves of the composition with $x = 0.03$ at different temperatures.

in the S–P^2, that means this composition is not an pure electrostrictive material at room temperature. Similar electrostrictive effect have been observed in the compositions with $x = 0.03$ but with decreased strain of 0.13%, as shown in Fig. 7. Especially, it is noted that for this composition, the room temperature S–P^2 curve is linear, indicating the room temperature electrostrictive effect of this composition.

4. Conclusions

In conclusion, $(1 - x)$BST–xBA ceramics have been synthesized and investigated, the solution limit is identified close to $x = 0.04$. A morphotropic phase boundary separating tetragonal and pseudocubic phases exists near $x = 0.02$, which corresponds to a transition from ferroelectric phase to a nonpolar phase. Pure electrostrictive effect can be observed with the strain level of 0.16%. Our results might be helpful for developing BST-based ceramics.

Acknowledgements

This work was supported by the National Nature Science Foundation of China (11174127, 11134006), the Doctoral Fund of Ministry of Education of China (20110091110014), the Nature Science Foundation of Jiangsu Province (No. BK2009007), and the Priority Academic Program Development of Jiangsu Higher Education Institutions.

References

[1] S.E. Park, T.R. Shrout, Ultrahigh strain and piezoelectric behavior in relaxor based ferroelectric single crystals, J. Appl. Phys. 82 (1997) 1084.
[2] J. Rödel, W. Jo, K.T.P. Seifert, E.-M. Anton, T. Granzow, Perspective on the development of lead-free piezoceramics, J. Am. Ceram. Soc. 92 (2009) 1153.
[3] T. Takenaka, H. Nagata, Y. Hiruma, Current developments and prospective of lead-free piezoelectric ceramics, Jpn. J. Appl. Phys. 47 (2008) 3787.
[4] W.M. Zhu, Z.-G. Ye, Ternary $Pb(Yb_{1/2}Nb_{1/2})O_3$–$PbZrO_3$–$PbTiO_3$ system as high-T_C/high-piezoelectric materials, Ceram. Int. 30 (2004) 1443.
[5] K. Kurihara, M. Kondo, High-strain piezoelectric ceramics and applications to actuators, Ceram. Int. 34 (2008) 695.
[6] http://ceramics.org/ceramictechtoday/2010/04/28/electrostrictive-ceramic-actuators-to-shape-mirror-of-next-space-telescope/2012-02-20.
[7] C. Ang, Z. Yu, High, purely electrostrictive strain in lead-free dielectrics, Adv. Mater. 18 (2006) 103.
[8] S.T. Zhang, A.B. Kounga, W. Jo, C. Jamin, K. Seifert, T. Granzow, J. Rödel, D. Damjanovic, High-strain lead-free antiferroelectric electrostrictors, Adv. Mater. 21 (2009) 4716.
[9] J.J. Wang, F.Y. Meng, X.Q. Ma, M.X. Xu, L.Q. Chen, Lattice, elastic, polarization, and electrostrictive properties of $BaTiO_3$ from first-principles, J. Appl. Phys. 108 (2010) 034107.
[10] A.K. Nath, K.C. Singh, R. Laishram, O.P. Thakur, Ferroelectric, piezoelectric and electrostrictive properties of $Ba(Ti_{1-x}Sn_x)O_3$ ceramics obtained from nanocrystalline powder, Mater. Sci. Eng. B 172 (2010) 151.
[11] H.V. Alexandru, C. Berbecaru, A. Ioachim, M.I. Toacsen, M.G. Banciu, L. Nedelcu, D. Ghetu, Oxides ferroelectric (Ba, Sr)TiO_3 for microwave devices, Mater. Sci. Eng. B 109 (2004) 152.
[12] H. Abdelkefi, H. Khemakhem, G. Velu, J.C. Carru, R.V. Muhll, Dielectric properties and ferroelectric phase transitions in $Ba_xSr_{1-x}TiO_3$ solid solution, J. Alloy Compd. 399 (2005) 1.

[13] J.W. Liou, B.S. Chiou, Dielectric characteristics of doped $Ba_{1-x}Sr_xTiO_3$ at the paraelectric state, Mater. Chem. Phys. 51 (1997) 59.
[14] B. Wu, L.Y. Zhang, X. Yao, Low temperature sintering of $Ba_xSr_{1-x}TiO_3$ glass–ceramic, Ceram. Int. 30 (2004) 1757.
[15] L. Szymczak, Z. Ujma, J. Handerek, J. Kapusta, Sintering effects on dielectric properties of (Ba,Sr)TiO_3 ceramics, Ceram. Int. 30 (2004) 1003.
[16] B. Zhang, X. Yao, L.Y. Zhang, Study on the structure and dielectric properties of BaO–SiO_2–B_2O_3 glass-doped (Ba,Sr)TiO_3 ceramics, Ceram. Int. 30 (2004) 1767.
[17] A.A. Belik, T. Wuernisha, T. Kamiyama, K. Mori, M. Maie, T. Nagai, Y. Matsui, E. Takayama-Muromachi, High-pressure synthesis, crystal structures, and properties of perovskite-like $BiAlO_3$ and pyroxene-like $BiGaO_3$, Chem. Mater. 18 (2006) 133.
[18] R.Z. Zuo, D.Y. Lv, J. Fu, Y. Liu, L.T. Li, Phase transition and electrical properties of lead free $(Na_{0.5}K_{0.5})NbO_3$–$BiAlO_3$ ceramics, J. Alloy Compd. 476 (2009) 836.
[19] A. Ullah, C.W. Ahn, A. Hussain, S.Y. Lee, I.W. Kim, Phase transition, electrical properties, and temperature-insensitive large strain in $BiAlO_3$-modified $Bi_{0.5}(Na_{0.75}K_{0.25})_{0.5}TiO_3$ lead-free piezoelectric ceramics, J. Am. Ceram. Soc. 94 (2011) 3915.
[20] H.C. Yu, Z.G. Ye, Dielectric properties and relaxor behavior of a new $(1-x)BaTiO_3$–$xBiAlO_3$ solid solution, J. Appl. Phys. 103 (2008) 034114.
[21] X.F. Liang, W.B. Wu, Z.Y. Meng, Dielectric and tunable characteristics of barium strontium titanate modified with Al_2O_3 addition, Mater. Sci. Eng. B 99 (2003) 366.
[22] X.S. Wang, H. Yamada, C.-N. Xu, Large electrostriction near the solubility limit in $BaTiO_3$–$CaTiO_3$ ceramics, Appl. Phys. Lett. 86 (2005) 022905.
[23] K.T.P. Seifert, W. Jo, J. Rödel, Temperature-insensitive large strain of $(Bi_{1/2}Na_{1/2})TiO_3$–$(Bi_{1/2}K_{1/2})TiO_3$–$(K_{0.5}Na_{0.5})NbO_3$ lead-free piezoceramics, J. Am. Ceram. Soc. 93 (2010) 1392.
[24] C. Ang, Z. Yu, High remnant polarization in $(Sr_{0.7}Bi_{0.2})TiO_3$–$(Na_{0.5}Bi_{0.5})TiO_3$ solid solutions, Appl. Phys. Lett. 95 (2009) 232908.
[25] S.T. Zhang, F. Yan, B. Yang, W.W. Cao, Phase diagram and electrostrictive properties of $Bi_{0.5}Na_{0.5}TiO_3$–$BaTiO_3$–$K_{0.5}Na_{0.5}NbO_3$ ceramics, Appl. Phys. Lett. 97 (2010) 122901.
[26] S.T. Zhang, A.B. Kounga, E. Aulbach, W. Jo, T. Granzow, H. Ehrenberg, J. Rödel, Lead-free piezoceramics with giant strain in the system $Bi_{0.5}Na_{0.5}TiO_3$–$BaTiO_3$–$K_{0.5}Na_{0.5}NbO_3$. II. Temperature dependent properties, J. Appl. Phys. 103 (2008) 034108.
[27] W. Jo, T. Granzow, E. Aulbach, J. Rödel, D. Damjanovic, Origin of the large strain response in $(K_{0.5}Na_{0.5})NbO_3$-modified $(Bi_{0.5}Na_{0.5})TiO_3$–$BaTiO_3$ lead-free piezoceramics, J. Appl. Phys. 105 (2009) 094102.
[28] Y. Hiruma, H. Nagata, T. Takenaka, Detection of morphotropic phase boundary of $(Bi_{1/2}Na_{1/2})TiO_3$–$Ba(Al_{1/2}Sb_{1/2})O_3$ solid-solution ceramics, Appl. Phys. Lett. 95 (2009) 052903.
[29] S.T. Zhang, A.B. Kounga, E. Aulbach, T. Granzow, W. Jo, H.-J. Kleebe, J. Rödel, Lead-free piezoceramics with giant strain in the system $Bi_{0.5}Na_{0.5}TiO_3$–$BaTiO_3$–$K_{0.5}Na_{0.5}NbO_3$. I. Structure and room temperature properties, J. Appl. Phys. 103 (2008) 034107.